

# Symmetrical short-period and high signal-to-noise ratio heterodyne grating interferometer

Cunbao Lin (林存宝), Shuhua Yan (颜树华)\*, Zhiguang Du (杜志广),  
Guochao Wang (王国超), and Chunhua Wei (魏春华)

College of Mechatronic Engineering and Automation, National University of Defense Technology,  
Changsha 410073, China

\*Corresponding author: yanshuhua996@163.com

Received June 9, 2015; accepted July 23, 2015; posted online August 31, 2015

A symmetrical heterodyne grating interferometer with both a short period and high signal-to-noise ratio is proposed. It possesses good immunity to environmental disturbances and can simultaneously achieve high resolution and stability. The experimental results show that the standard deviation of 24.67 nm can be realized for the long range of 10 mm. The measurement resolution of better than 2 nm is achieved with the theoretical resolution of 12 pm. Additionally, system stability at less than  $\pm 1.5$  nm is obtained in just over 10 min. The measurement errors, including cosine error, nonlinear error and non-common path error, are discussed as well.

OCIS codes: 050.1950, 120.3180, 120.3930.

doi: 10.3788/COL201513.100501.

Precision displacement measurement plays an important role in modern industry. With the capacity of environment insensitivity and its cost effectiveness compared with traditional laser interferometers, grating interferometers (GIs) have been widely used in variety of fields<sup>[1,2]</sup>. The symmetrical optical configurations are perhaps the most popular arrangements in GIs, since they usually exhibit better immunity to environmental disturbances. Meanwhile, since the achievable measurement resolution is considered to mainly depend on the period of the signal and the signal-to-noise ratio (SNR)<sup>[3,4]</sup>, gratings with a short period and high diffraction efficiency are greatly favored in high-precision GIs. For one thing, the short period is beneficial to improving the resolution and depressing the errors<sup>[5]</sup>. For another, the high diffraction efficiency always leads to a high SNR, which is able to obtain higher accuracy for the phase measurement<sup>[4,6]</sup>. However, gratings with a shorter period often exhibit serious polarization dependency<sup>[7]</sup>. The different diffraction efficiencies between TE and TM polarization would severely decline the SNR of the measurement signals, and sometimes would even bring interpolation errors<sup>[8]</sup>. The GIs with both a short period and a high SNR would be attractive in practical applications.

Both homodyne- and the heterodyne-type GIs have been proposed for displacement measurement. With the introduction of a carrier, heterodyne grating interferometers (HGIs) overcome the direct current offset and the amplitude variation of the measurement signals that the homodyne type always encounters<sup>[9]</sup>. Lee *et al.* first proposed a HGI with subnanometric resolution<sup>[10]</sup>; then, they introduced the shearing interferometry into HGIs for long-range applications<sup>[11]</sup>. Wu *et al.* presented a HGI with a double-diffraction arrangement that can effectively compensate the head-to-scale error<sup>[5]</sup>, then developed a common-path HGI with a Littrow configuration to further

improve the resolution and stability<sup>[9]</sup>. Hsieh *et al.* proposed a HGI with a quasi-common-optical-path configuration<sup>[12]</sup>. Hsu *et al.* presented a HGI with holographic gratings and integrated it into a compact displacement sensor<sup>[13]</sup>. Although these HGIs often exhibit remarkable performance with specific merits, the one that simultaneously concentrates on the short period and high SNR has rarely been reported for displacement measurement.

In this Letter, we propose a symmetrical HGI with both a short period and high SNR. The short-period scale grating is especially utilized to decrease the signal period and improve the diffraction efficiency. Meanwhile, a half-wave plate (HWP) arrangement is adopted to enhance the SNR and the contrast of the measurement signals. With the simultaneous modification of the effects of the optical and the electronic systems, the overall performance of the HGI is expected to be effectively improved. In the remainder of this paper, the measurement principle of the proposed HGI is presented first. Then, the performance testing, including the long-range, short-range, and stability measurements, are discussed, including a comparison of the calibration equipment. Finally, the cosine error, nonlinear error, and non-common path (NCP) error of the HGI are discussed.

The schematic of the proposed HGI is shown in Fig. 1. A dual-frequency laser (L) emits two orthogonally linear polarizations,  $p$  and  $s$ , with the frequency of  $f_1$  and  $f_2$ , respectively. They are incident on a beam splitter and are divided into two parts, one for reference and the other for measurement. The reference beam passes through a polarizer (P) with a transmittance axis at  $45^\circ$ . Then, it is received by the photodetector  $D_r$ , and the reference signal is generated. The measurement beam is incident on a polarizing beam splitter (PBS), and the two polarizations are separated. Then, one of the polarizations is changed into the other by a HWP with a transmittance axis at

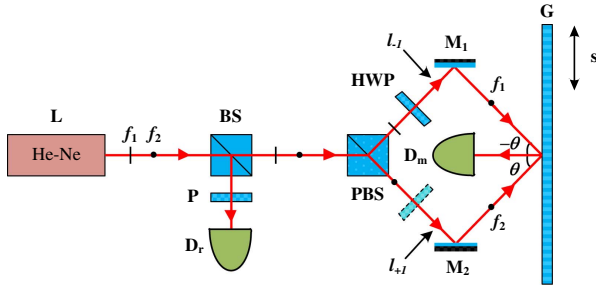


Fig. 1. Schematic of the optical configuration for the proposed HGI, BS: beam splitter.

$45^\circ$ . Both of the beams are reflected by the mirrors ( $M_{1,2}$ ), and are incident on the grating (G) at the first-order diffraction angle  $\theta$ . The  $+1$  and the  $-1$  order diffraction beams overlap and they emit perpendicular to the grating surface. They are received by the photodetector  $D_m$ , and the measurement signal is then generated.

According to the Jones matrix, the light emitting from the dual-frequency laser can be expressed as

$$E_0 = \begin{bmatrix} 1 \\ 0 \end{bmatrix} \exp(i\omega_1 t) + \begin{bmatrix} 0 \\ 1 \end{bmatrix} \exp(i\omega_2 t), \quad (1)$$

where  $\omega_1 = 2\pi f_1$  and  $\omega_2 = 2\pi f_2$  are the angular frequencies of the two polarizations, respectively. The reference signal that is received by the photodetector  $D_r$  can be written as

$$I_r \propto \cos[(\omega_1 - \omega_2)t]. \quad (2)$$

For the measurement signal, it would have a different expression if the HWP were placed on a different path. When the HWP is placed on the path of the  $p$  polarization, the measurement signal can be written as

$$I_{ms} \propto \eta_s(\theta) \cdot \cos[(\omega_1 - \omega_2)t + k(l_{-1} - l_{+1}) + (\phi_{-1} - \phi_{+1})]. \quad (3)$$

Meanwhile, if the HWP is placed on the path of the  $s$  polarization, the measurement signal can be expressed as

$$I_{mp} \propto \eta_p(\theta) \cdot \cos[(\omega_1 - \omega_2)t + k(l_{-1} - l_{+1}) + (\phi_{-1} - \phi_{+1})], \quad (4)$$

where  $\eta_s(\theta)$  and  $\eta_p(\theta)$  denote the diffraction efficiencies of the grating for the  $s$  and the  $p$  polarizations, respectively.  $k$  denotes the wave vector in air and is defined as  $2\pi n/\lambda$ ,  $n$  is the air refractive index,  $l_{-1}$  and  $l_{+1}$  represent the lengths of the two separate paths resulting from the NCP configuration, and  $\phi_{-1}$  and  $\phi_{+1}$  represent the phase shifts of the  $\pm 1$  order diffraction beams varying with the grating's movement. When the grating undergoes a displacement of  $s$ ,  $\phi_{-1}$  and  $\phi_{+1}$  can be obtained with

$$\phi_{\pm 1} = \pm 2\pi s/d, \quad (5)$$

where  $d$  is the grating pitch. It can be seen from Eqs. (3) and (4) that the amplitude of the measurement signal is proportional to the diffraction efficiency of the grating. Since gratings often have different diffraction efficiencies for the  $s$  and the  $p$  polarizations, the place of the HWP should be deliberately chosen in the proposed HGIs. If the grating has a higher diffraction efficiency for the  $s$  polarization, the HWP should be placed on the  $l_{-1}$  path to change the  $p$  polarization into the  $s$  polarization; otherwise, it should be placed on the  $l_{+1}$  path to change the  $s$  polarization into the  $p$  polarization. Then the polarization with the higher diffraction efficiency can be utilized, and the SNR of the measurement signal would also be enhanced.

After the optical signals are converted to the electronic signals, they are sent into a phasemeter or a lock-in amplifier, and the phase difference  $\phi_{\text{mea}}$  between the reference signal and the measurement signal can be measured as

$$\phi_{\text{mea}} = \phi_{\text{non}} + \phi_{\text{mov}} = k(l_{-1} - l_{+1}) + (\phi_{-1} - \phi_{+1}), \quad (6)$$

where  $\phi_{\text{non}}$  and  $\phi_{\text{mov}}$  are the phase differences resulting from the NCP configuration and the grating movement, respectively. The result reveals that the NCP phase difference is mainly determined by the wave vector and the length difference of the two paths. With the symmetrical optical configurations, even though the errors resulting from the atmospheric inhomogeneity and thermal effect cannot be suppressed, the part owing to the uniform change of the air refractive index could be effectively decreased. If the NCP phase difference  $\phi_{\text{non}}$  is assumed to be a constant and ignored, then the grating displacement  $s$  can be obtained as

$$s = \frac{\phi_{\text{mea}}}{4\pi} \cdot d. \quad (7)$$

This equation reveals that the displacement is proportional to the measured phase difference and the grating pitch. When the short-period grating is utilized, the sensitivity would be enhanced and the errors would also be depressed. Then, the resolution and stability of the HGI would also be improved. Additionally, compared with other HGIs, with the cooperating utilization of the short-period scale grating and the HWP arrangement, the short period and high SNR would be simultaneously obtained. Then the effects of both the optical and the electronic systems would be improved. Therefore, the high resolution and stability are more likely to be achieved for the proposed HGI.

A dual-frequency laser (model: 5519A, Agilent Inc.) with a nominal vacuum wavelength of 632.991 nm was used as the light source, as shown in Fig. 2. All the optical components were mounted with on short pedestals to minimize the volume and enhance the steadiness<sup>[2]</sup>. A reflective holographic grating (model: GH25-12 V, Thorlabs Inc.) with a short period of 833 nm was utilized as the

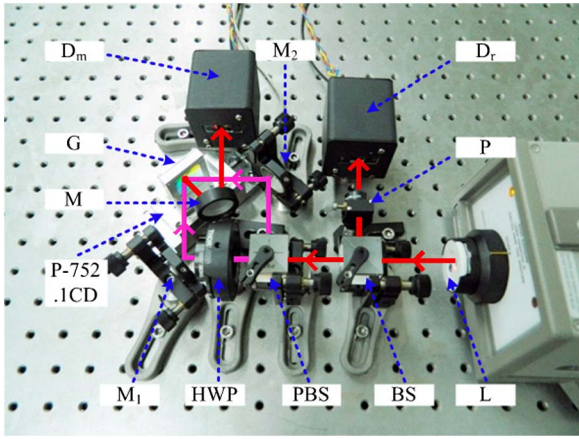


Fig. 2. Experimental setup of the optical system for the proposed HGI.

measurement scale. The diffraction efficiencies for the  $p$  and the  $s$  polarizations are 40% and 60% under the Littrow configuration, respectively. Therefore, the HWP is placed on the  $l_{-1}$  path to change the  $p$  polarization into an  $s$  polarization to improve the SNR of the measurement signal. The grating was fixed on a 15  $\mu\text{m}$ -range piezoelectric stage (model: P-752.1CD, Physik Instrumente Inc.) with a specially designed mounting device. A motorized stage (model: KSA150-12-X, Zolix Inc.) with a range of 150 mm was also used for a long-range experiment. A laser interferometer (model: XL-80, Renishaw Inc.) with resolution of 1 nm was utilized to monitor the displacement of the stage. The detection signals were sent to the lock-in amplifier (model: SR830, Stanford Research Systems Inc.) and our homemade phasemeter to measure the phase difference. The system was constructed in a clean room on the first underground floor, and the optical layout was shielded by enclosures during the experiments.

The long-range measurement capability of the proposed HGI was tested using millimeter-scale displacements. The motorized stage was used to move the grating, and a modified homemade phasemeter with resolution of  $0.18^\circ$ <sup>[14]</sup> was utilized to measure the phase difference. The motorized stage was set to make a round-trip movement ten times with a displacement of 10 mm. The actual displacement of the grating was monitored by the XL-80. Figure 3 shows the measurement results of the HGI and the XL-80. The different slopes between the first- and the second-half sections for the forward and the backward movements are attributed to the unequal moving speed of the motorized stage. The inset in Fig. 3 shows that a difference of about 1.2  $\mu\text{m}$  is observed for the 10 mm displacement. This mainly results from the cosine error, which results from the discrepancy between the grating vector and the optical axis of the XL-80. We averaged the measurement results for ten seconds after the stage recovers and stabilizes; the averages of the HGI and the XL-80 are listed in Table 1. The ratios between the HGI and the XL-80 are calculated as well. Since the movement of the grating was taken at the same position as the KSA150-12-X stage, the cosine

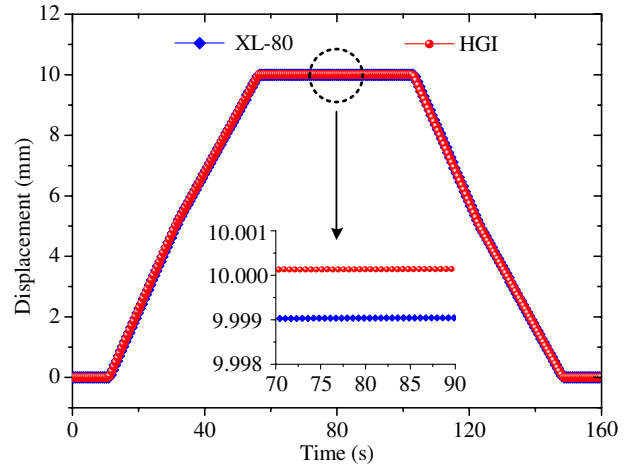


Fig. 3. Measurement result of the linear movement with a displacement of 10 mm.

errors are assumed to be the same for all ten measurements. Then, the mean value of 1.000119 for these ratios is calculated and is set to be the correction factor for the cosine errors. The residual errors after the cosine errors have been removed using the correction factor<sup>[15]</sup> are exhibited in Table 1. It reveals that the residual error for the 10 mm displacement is within  $\pm 50$  nm, and the standard deviation is calculated to be 24.67 nm.

The short-range measurement capability of the proposed HGI was tested with micron and nanometer scale displacements. The P-752.1CD piezoelectric stage with a resolution of 0.1 nm was used to provide the movement of the grating. In combination with frequency down-conversion technology, the SR830 lock-in amplifier with a phase resolution of  $0.01^\circ$  was utilized to measure the phase difference. The theoretical resolution of the HGI corresponding to  $0.01^\circ$  phase resolution is 12 pm. First, the P-752.1CD stage was set to move in a sinusoidal

**Table 1.** Measurement Results and Residual Errors of the HGI and the XL-80 for the 10 mm Displacement

	HGI (mm)	XL-80 (mm)	Ratio	Residual Error (nm)
1st	10.000710	9.999553	1.000116	-32.95
2nd	10.000657	9.999463	1.000120	4.07
3rd	10.000142	9.998967	1.000118	-14.88
4th	10.000943	9.999773	1.000117	-19.97
5th	10.000125	9.998907	1.000122	28.13
6th	10.000241	9.999100	1.000114	-48.89
7th	10.000400	9.999201	1.000120	9.10
8th	10.000747	9.999537	1.000121	20.06
9th	10.000079	9.998900	1.000118	-10.87
10th	10.000453	9.999236	1.000122	27.09

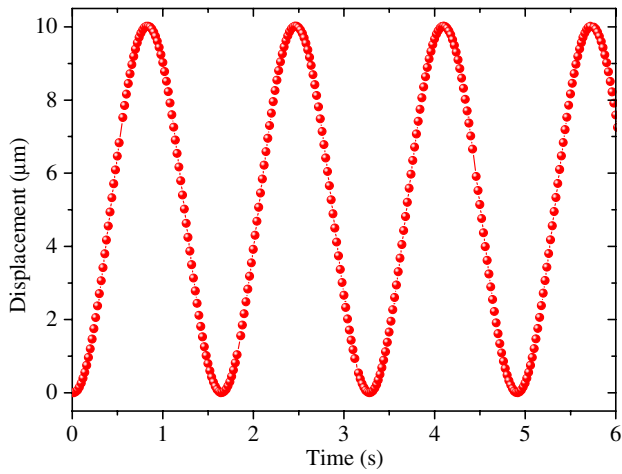


Fig. 4. Measurement result of the sinusoidal movement with an amplitude of  $10\ \mu\text{m}$ .

displacement with an amplitude of  $10\ \mu\text{m}$ . Figure 4 shows the measurement result of the HGI, which is quite close to the ideal sinusoidal wave. The peak-to-peak value of the measured sinusoidal displacement is  $10.015\ \mu\text{m}$ , which is a little bigger than the set value of  $10\ \mu\text{m}$ . This discrepancy is considered to be mainly from the cosine error. Then, the P-752.1CD stage was set to make a  $10\ \text{nm}$ -step movement in  $2\ \text{nm}$  steps. Both the forward and backward movements were conducted to simultaneously test the repeatability of the HGI. Figure 5 shows the measurement result of the HGI for the round-trip step movement. It illustrates that the  $2\ \text{nm}$  step movement can be clearly detected by the HGI, which means the measurement resolution is better than  $2\ \text{nm}$ . With the definition of repeatability given in Ref. [16], the repeatability of the proposed HGI is calculated to be about  $0.25\ \text{nm}$ .

The stability of the proposed HGI was then tested and compared with that of the XL-80 laser interferometer. The P-752.1CD stage was turned off electrically to remove the piezoelectric deformation. The XL-80 laser interferometer

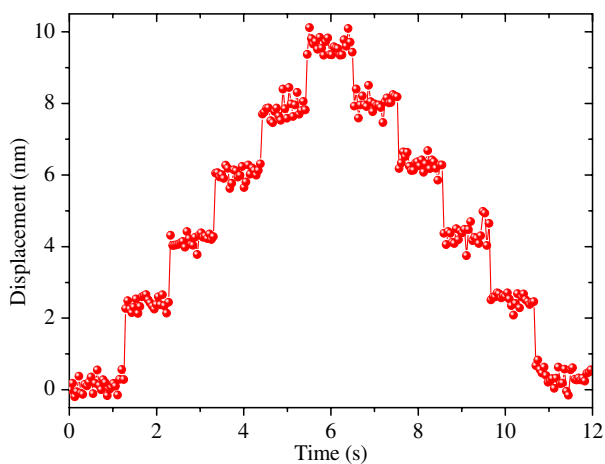


Fig. 5. Measurement result of the round-trip step movement with a total displacement of  $10\ \text{nm}$ .

was fixed next to the HGI, and they were shielded into the same space. We simultaneously initialized these two instruments and set them to detect the displacement variation for ten minutes. Figure 6 shows the stability measurement results for the HGI and the XL-80. It indicates that the fluctuation of the HGI is within  $\pm 1.5\ \text{nm}$  and no evident drift is observed, whereas the stability of the XL-80 is about  $20\ \text{nm}$  and suffers from drift. The results reveal that the HGI has better immunity to the drift effect than the XL-80. The symmetrical configuration and miniaturized volume are considered to be the dominant reasons for the good stability compared with the laser interferometer.

Among these error sources for the proposed HGI, the cosine error perhaps is the most important one. It mainly results from the misalignment of the optical components. As illustrated in the above measurement results, the relative deviations are about  $15\ \text{nm}$  and  $1.2\ \mu\text{m}$  for the short- and long-range displacement measurements, respectively. It is consistent with the theoretical derivation, since the cosine error is directly proportional to the measurement displacement. These errors can be greatly declined with the proper alignment in displacement measurement<sup>[17]</sup>.

The nonlinear error is also a dominant error source for the proposed HGI. The nonorthogonality and ellipticity of the dual-frequency laser, the imperfect extinction ratio of the PBS, and the inaccurate azimuth angle of the HWP, all result in the frequency mixing, polarization mixing, and polarization-frequency mixing errors. Based on our previous analysis<sup>[18]</sup>, with the nonorthogonal angle, the ellipticity, the extinction ratio, and the inaccurate azimuth angle of about  $1^\circ$ ,  $0.08$ ,  $0.01\%$ , and  $1^\circ$  in our system, the frequency mixing, polarization mixing, and polarization-frequency mixing errors are estimated to be  $1.15$ ,  $0.01$ , and  $0.42\ \text{nm}$ , respectively. Therefore, the maximum nonlinear error in our system is about  $1.58\ \text{nm}$ . The passive approach can be applied to compensate for these nonlinear errors<sup>[19]</sup>.

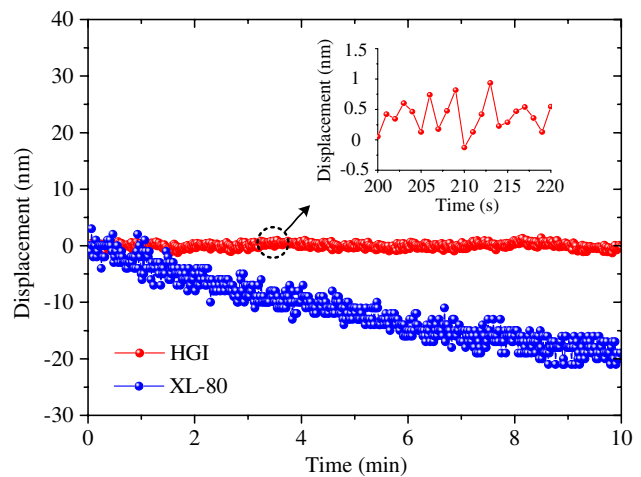


Fig. 6. Stability measurement results for the HGI and the XL-80 in ten minutes.



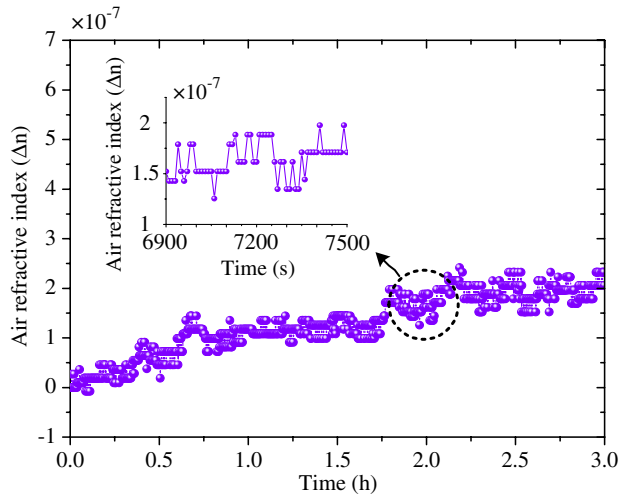


Fig. 7. Variation of the air refractive index in 3 h.

The NCP error, which results from the non-overlap of the two optical paths  $L_{-1}$  and  $L_{+1}$ , is another error for the proposed HGI. Since the symmetrical optical configuration is utilized in our HGI, the difference between  $L_{-1}$  and  $L_{+1}$  was measured to be less than 5 mm. The air refractive index was also monitored by an air sensor (model: E1738A, Agilent Inc.) with the temperature, humidity, and pressure resolutions being  $0.01^\circ$ , 1%, and 10 Pa, respectively. The total air temperature, humidity, and pressure changes were detected to be  $0.05^\circ$ , 3%, and 90 Pa within three hours. The variation of the air refractive index was then calculated with the modified Edlén equation<sup>[20]</sup>, and is shown in Fig. 7. It reveals that the variations of the air refractive index are within  $3 \times 10^{-7}$  in 3 h and within  $1 \times 10^{-7}$  in 10 min. If the gradient of the air refractive index is ignored, the variation of the displacement would be about 0.5 nm within 10 min. Since the stability of the proposed HGI is about  $\pm 1.5$  nm, the remaining errors resulting from the material thermal expansion, background vibration, and electronics noises also need to be analyzed to further improve the performance of the HGI.

In conclusion, we propose a symmetrical HGI with both a short period and a high SNR. The resolution and stability are effectively improved with the specially designed optical configuration. The experimental results show that the proposed HGI can simultaneously achieve nanometer resolution and millimeter range, which means it is

appropriate for both high-resolution and long-range displacement measurements. Additionally, the stability of the HGI is tested, and it exhibits better immunity than the laser interferometer. It reveals that it is more suitable for applications in the ordinary environment. The cosine error, nonlinear error, and NCP error are also analyzed for the proposed HGI. Our future work will mainly involve compensating for the measurement errors to further improve the performance of the HGI.

This work was supported by the National Natural Science Foundation of China under Grant No. 51275523.

## References

1. Y. Fu, J. Yang, Z. Wang, and H. Wu, *Chin. Opt. Lett.* **12**, 121101 (2014).
2. H. L. Hsieh and S. W. Pan, *Opt. Express* **23**, 2451 (2015).
3. E. Higurashi and R. Sawada, *J. Micromech. Microeng.* **15**, 1459 (2005).
4. T. Hausotte, B. Percle, U. Gerhardt, D. Dontsov, E. Manske, and G. Jäger, *Meas. Sci. Technol.* **23**, 074004 (2012).
5. C. C. Wu, C. C. Hsu, J. Y. Lee, H. Y. Chen, and C. L. Dai, *Meas. Sci. Technol.* **19**, 045305 (2008).
6. Z. Huang, C. Li, and X. Sun, *Chin. Opt. Lett.* **11**, 091203 (2013).
7. C. B. Lin, S. H. Yan, Z. G. Du, C. H. Wei, and G. C. Wang, *Opt. Commun.* **339**, 86 (2015).
8. C. K. Lee, C. C. Wu, S. J. Chen, L. B. Yu, Y. C. Chang, Y. F. Wang, J. Y. Chen, and J. W. Wu, *Appl. Opt.* **43**, 5754 (2004).
9. C. C. Wu, C. C. Hsu, J. Y. Lee, and Y. Z. Chen, *Opt. Express* **21**, 13322 (2013).
10. J. Y. Lee, H. Y. Chen, C. C. Hsu, and C. C. Wu, *Sens. Actuators A* **137**, 185 (2007).
11. J. Y. Lee and M. P. Lu, *Opt. Commun.* **284**, 857 (2011).
12. H. L. Hsieh, J. Y. Lee, W. T. Wu, J. C. Chen, R. Deturche, and G. Lerondel, *Meas. Sci. Technol.* **21**, 115304 (2010).
13. C. C. Hsu, Y. Y. Sung, Z. R. Lin, and M. C. Kao, *Opt. Laser Technol.* **48**, 200 (2013).
14. G. C. Wang, S. H. Yan, W. H. Zhou, and C. H. Gu, *Opt. Eng.* **51**, 081512 (2012).
15. F. Chen and K. C. Fan, *Appl. Opt.* **50**, 4550 (2011).
16. L. Chassagne, M. Wakim, S. Xu, S. Topcu, P. Ruaux, P. Juncar, and Y. Alayli, *Meas. Sci. Technol.* **18**, 3267 (2007).
17. S. Wang, Z. Li, Y. Huang, G. Lin, and X. Yang, *Chin. Opt. Lett.* **13**, S11202 (2015).
18. C. B. Lin, S. H. Yan, C. H. Wei, G. C. Wang, and P. F. Zou, *Proc. SPIE* **9046**, 90460C (2013).
19. J. Ahn, J. A. Kim, C. S. Kang, J. W. Kim, and S. Kim, *Opt. Express* **17**, 23300 (2009).
20. K. P. Birch and M. J. Downs, *Metrologia* **31**, 315 (1994).